Publication VI

$$\boxed{\text{VI}}$$

An Air Distribution Index for Assessing the Thermal Comfort and Air Quality in Uniform and Nonuniform Thermal Environments

I. Almesri[a,b]   H. B. Awbi[a]   E. Foda[c]   K. Sirén[c]

[a]School of Construction Management and Engineering, University of Reading, Reading, UK
[b]Department of Mechanical Engineering, College of Technological Studies, Kuwait
[c]Department of Energy Technology, Aalto University, Espoo, Finland

Key Words

Air distribution index · Room air distribution · Ventilation systems · Local thermal comfort · Virtual thermal manikin · Computational fluid dynamics

Abstract

This study introduces a new Air Distribution Index $(ADI)_{New}$ to assess the ventilation performance in uniform and nonuniform thermal environments. The index comprises parameters for assessing the indoor thermal comfort and air quality in occupied spaces. The thermal comfort assessment was carried out using a virtual thermal manikin that is adjusted by a model of human thermoregulation and coupled with a psychological comfort model. The virtual manikin was used in a computational fluid dynamics (CFD) code to simulate tests in an environmental chamber that were largely conducted under thermally neutral conditions with mixing ventilation (MV) or displacement ventilation (DV) systems. Eight human subjects were used in the study that included measurement of their skin temperature, local and overall thermal sensation votes during their exposure to the MV and DV systems. The results from CFD predictions were compared with measurements in the test chamber. The predicted $(ADI)_{New}$ parameters, such as the thermal comfort, the ventilation effectiveness for both heat and contaminant removals as well as the local mean age of air, were compared with measured values in the chamber and found to be in good agreement. The results demonstrate that $(ADI)_{New}$ is a useful index for evaluating the performance of a ventilation system under uniform thermal environment and can also be applied to nonuniform environment.

Introduction

The main purpose of a ventilation system is to provide thermal comfort to occupants as well as improve the indoor air quality by removing pollutants generated in rooms. In the past, these two parameters (i.e. thermal comfort and air quality) have been examined separately in evaluating an air distribution system performance.

Dr Hazim B. Awbi,
School of Construction Management and Engineering, University of Reading, Reading, UK
E-mail h.b.awbi@reading.ac.uk

Many studies have investigated the performance of ventilation systems for providing thermal comfort [1–3] and others have focused on the ability of a ventilation system in removing indoor pollutants [4–7]. However, a ventilation system may be effective in providing good air quality but could be less effective in providing thermal comfort and energy performance and vice versa. Therefore, it is beneficial to develop a method to assess the ventilation performance in providing both thermal comfort and air quality. Awbi and Gan [8] and Awbi [9] developed the concept of the ventilation parameter (*VP*), which was later renamed the air distribution index (*ADI*) [10,11]. The *ADI* represents a holistic approach for assessing the thermal comfort, indoor air quality and energy performance of an air distribution system. Since the thermal comfort part of the *ADI* was based on Fanger's *PMV* model [12], the *ADI* is applicable to and can be effective for evaluating the performance of a ventilation system that creates a uniform environment but it could be less accurate for evaluating systems that create nonuniform thermal environments. However, in practice the majority of indoor environments are seldom uniform. Hence, this study proposes a new air distribution index (*ADI*)$_{New}$ which can be applicable for the assessment of ventilation systems that provide either uniform or nonuniform thermal environments.

The concept of local thermal comfort that corresponds to body segments underlies the thermal prediction for the whole body and represents the current state-of-the-art in the prediction of the thermal comfort of individuals. The prediction of thermal comfort that is based on local effects accounts for the nonuniformity in the thermal environments. Generally, the prediction of local thermal comfort is based on the local skin temperatures as stipulated in the concept of the equivalent (homogeneous) temperature [13] and the use of a comfort model such as the University of California, Berkeley (UCB) model [14]. Therefore, the multisegmental physiological (thermoregulation) models which can predict local skin temperatures along with other physiological variables have gained more importance with the local thermal comfort concept. Such models of human thermoregulation can be used to predict the local skin temperature, hence evaluating the local thermal comfort of individuals. This methodology has not yet been adopted by any of the international standards and guidelines and needs further validations.

In an earlier study, the authors compared predictive methods of the human skin temperature and thermal sensations [15]. The multisegmental (MS) Pierce model [16] was coupled with the UCB comfort model to predict

the local comfort under different conditions obtained from the literature. Compared with subjective data, the results showed satisfactory predictions and were nearly in good agreement with predictions using the equivalent temperature (*t*eq) approach of Nilsson's model [17].

In this study, local subjective votes (based on the Bedford scale) from 45 different indoor conditions as given in two studies [17,18] were correlated with the predicted skin temperatures using the MS-Pierce model under the same test conditions. This was used to develop a local comfort model that was adapted from the UCB comfort model. The prediction of the overall thermal comfort was based on a weighted average of the local comfort predictions. A virtual manikin was constructed and used in the computational fluid dynamics (CFD) code VORTEX 4.0 [19] to predict the room environment. The virtual manikin simulated the occupant's presence in the room and was thermally adjusted using the MS-Pierce thermoregulation model. This simulation approach for the prediction of the (*ADI*)$_{New}$ was then tested against measured data for two cases in an environmental test chamber served by mixing and displacement ventilation systems.

Methods

New Air Distribution Index (ADI)$_{New}$

The proposed air distribution index (*ADI*)$_{New}$ combines the thermal comfort and air quality numbers as represented by Equation (1) [20,21]:

$$(ADI)_{New} = \underbrace{\left[\left(1 - \frac{|S|}{3}\right) * \varepsilon_t\right]}_{N_{T.C.}} + \underbrace{\left[\left(\frac{\tau_n}{\overline{\tau_p}}\right) * \varepsilon_c\right]}_{N_{A.Q.}} \qquad (1)$$

where $N_{T.C.}$ is the thermal comfort number, $N_{A.Q.}$ is the air quality number, $|S|$ is the absolute value of the average overall thermal sensation over the exposure time, ε_t is the ventilation effectiveness for heat removal, τ_n is the room time constant, $\overline{\tau_p}$ is the local mean age of air and ε_c is the ventilation effectiveness for contaminant removal. These parameters are calculated as shown by Equation (2):

$$\varepsilon_t = \frac{T_o - T_i}{T_m - T_i}, \varepsilon_c = \frac{C_o - C_i}{C_m - C_i}, \tau_n = \frac{1}{ACH} \qquad (2)$$

where T_o, T_i and T_m are the temperature at the outlet, at the inlet and the mean value in the occupied zone respectively; C_o, C_i and C_m are the contaminant (CO_2) concentrations at the same locations and *ACH* is the room

air change rate per hour. The local mean age of air is calculated using Equation (3):

$$\bar{\tau}_p = \frac{1}{C(0)} \int_0^\infty C_p(t)\mathrm{d}t \qquad (3)$$

where $C(0)$ is the initial concentration of a tracer gas and C_p is the gas concentration at a certain point in the room (e.g. breathing zone).

The logic beyond developing the $(ADI)_{\text{New}}$ in the manner shown in Equation (1) is that when the occupant's thermal sensation is neutral (i.e. $|S| = 0$), which is the ideal thermal condition, $N_{\text{T.C.}}$ reaches its maximum value and when $|S|$ reaches its extreme values (i.e. -3 or $+3$), $N_{\text{T.C.}}$ reaches its minimum value (zero). Also a high value of ε_t implies that the ventilation system is efficient in removing heat from the occupied zone. τ_n, $\bar{\tau}_p$ and ε_c are important factors that are incorporated for evaluating the air quality number in $(ADI)_{\text{New}}$ and consequently assessing the air distribution performance in an enclosed space. A high value of τ_n and ε_c and a low value of $\bar{\tau}_p$ mean that the ventilation system is good in removing contaminants as well as providing fresh air to the occupied zone. Therefore, the $(ADI)_{\text{New}}$ presented in the form shown in Equation (1) could be a useful tool for evaluating both thermal comfort (based on the local comfort concept) and air quality whether the thermal environment is uniform or nonuniform. Although $(ADI)_{\text{New}}$ does not represent an absolute measure of the performance of an air distribution system, the concept does however provide useful information on how a system is performing in terms of thermal comfort and indoor air quality provision. In principle, a high value of $(ADI)_{\text{New}}$ would mean good performance but in addition $N_{\text{T.C.}}$ and $N_{\text{A.Q.}}$ should have nearly equal values to ensure that the system provides thermal comfort and indoor air quality equally.

The Multisegmental (MS) Pierce Model

The MS-Pierce model [16] was developed on the basis of the original 2-node Pierce model [22] using: measured data in neutral condition to adjust the local skin set-points and to calculate the local core set-points (using a line search method) that allows the model to predict the skin temperatures in the neutral condition with high accuracy; a modified calculation procedure for the convective heat transfer coefficients; and adjustment to the heat transfer term from core to skin using a common blood temperature along with the local core temperatures. The model predictability was verified for steady-state and dynamic conditions using measured data at uniform neutral, cold and warm as well as several different asymmetric thermal conditions and produced an average absolute skin temperature deviation in the range of 0.3–0.8 K [15]. The model combines useful features such as simplicity along with a good accuracy in estimating the local skin temperatures.

In this study, the MS-Pierce model was used in the construction of the comfort model and for the regulation of the virtual manikin in the CFD simulations.

Thermal Comfort Model

Model Construction

The overall thermal comfort is estimated for the calculation of $(ADI)_{\text{New}}$ using a weighted average of the local thermal comfort perceived by the different body segments. The local comfort is predicted using a model that was adapted from the UCB local sensation model [14]. However, for the purpose of this research, the UCB model's proposed term for the impact of the overall sensation on body segments was not included for simplicity. Hence, the adapted model accounts only for the local skin temperature's deviation from its set-point value. In addition, a standard 7-point scale (Bedford scale) was used instead of the extended 9-point scale that is used with the UCB model (Figure 1). With this scale, when the local skin temperature deviates much from its set-point, the local comfort approaches its extreme values (i.e. -3, $+3$). The Bedford scale was used in earlier studies to asses both thermal sensation and comfort and may be seen in that sense as an inclusive good option to use for $(ADI)_{\text{New}}$.

The proposed local thermal comfort model has the following form as represented by Equation (4) [14]:

$$LTC = 3 * \left(\frac{2}{1 + EXP\left(-C * (T_{\text{skin, local}} - T_{\text{skin, local, set}})\right)} - 1 \right)$$
$$(4)$$

where LTC is the local thermal comfort (based on Bedford 7-point scale); C is a coefficient with a value between 0 and 1 that depends on the different body parts; $T_{\text{skin,local}}$ is the local skin temperature (°C); and $T_{\text{skin,local,set}}$ is its set-point (°C).

The regression coefficient C is obtained for each body segment from the correlation of the skin temperature deviation from its set-point against the subjective local comfort votes under defined conditions. In this study, this was carried out using subjective votes (Bedford scale) from two other studies [17,18] along with the predicted skin temperature's deviation by the MS-Pierce model using the test conditions from the same studies.
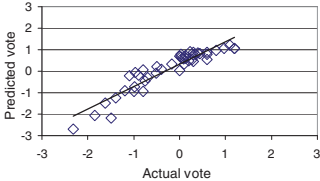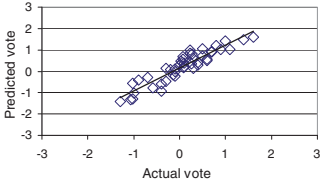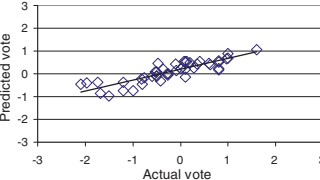
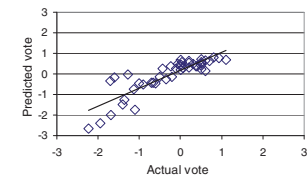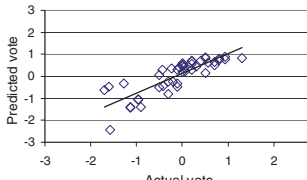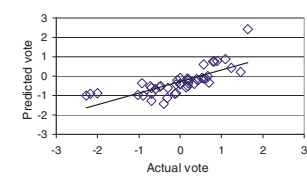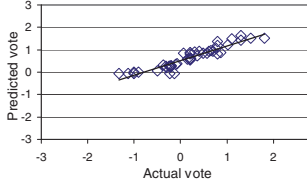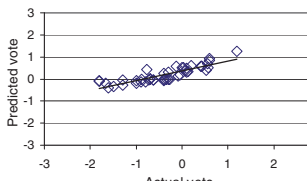**Fig. 1.** Bedford 7-point scale and the extended 9-point scale (UCB model).

Table 1. Local thermal comfort model coefficients and correlation with actual votes
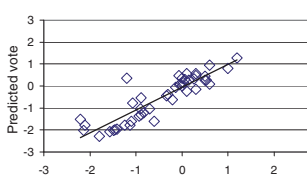
Segment	Regression coefficient, C		Coefficient of determination (R^2)	Actual vs Predicted
	$\Delta T < 0$	$\Delta T > 0$		
Head	0.14	0.85	0.46	
U. Back	0.47	0.55	0.75	
Chest	0.4	1	0.79	

Continued

Table 1. Continued

Segment	Regression coefficient, C		Coefficient of determination (R^2)	Actual vs Predicted
	$\Delta T < 0$	$\Delta T > 0$		
U. Arm	0.58	0.59	0.75	
L. Arm	0.72	0.55	0.69	
Hand	0.1	0.4	0.56	
Thigh	0.1	0.49	0.88	
L. Leg	0.1	0.83	0.75	
Foot	0.29	0.85	0.8	

Table 1. Continued

Segment	Regression coefficient, C		Coefficient of determination (R^2)	Actual vs Predicted
	$\Delta T < 0$	$\Delta T > 0$		
L. Back	0.65	0.61	0.86	
Abdomen	1	1	0.86	
Overall	NA	NA	0.75	

Nilsson [17] carried out experiments for 30 different climatic conditions using two thermal manikins to measure the heat flux for individual body segments and the measured local heat flux was used to calculate the segmental equivalent temperature. The equivalent temperatures obtained under these conditions were correlated with subjective votes from human subjects' tests under the same test conditions. The subjects (20 subjects for each condition) reported their local and overall thermal sensations on the Bedford scale. The individual votes were averaged for each test condition and reported as a mean thermal vote (MTV).

Cheong et al. [18] conducted human subjects' experiments under 15 different test conditions. This was carried out in a climatic chamber to investigate the local and overall thermal sensation and comfort in environments served with displacement ventilation. The tests were performed under different room air temperatures, different temperature gradients between ankle and head, and different clothing ensembles. In total, 60 male and female subjects participated in these tests (30 for each condition) in which they voted their thermal comfort perception on the Bedford scale.

The environmental parameters (i.e. air temperature, air velocity, radiant temperature and relative humidity) and the segmental clothing insulation values from the aforementioned studies [17,18] were entered into the MS-Pierce thermoregulation model [16] to predict the local skin temperatures. The predicted local skin temperatures were correlated with the actual local comfort votes to obtain the coefficient C for the different body segments. The coefficient C for each body segment was obtained for two cases: when the skin temperature deviation $\Delta T (= T_{\text{skin,local}} - T_{\text{skin,local,set}}) < 0$ and when $\Delta T > 0$.
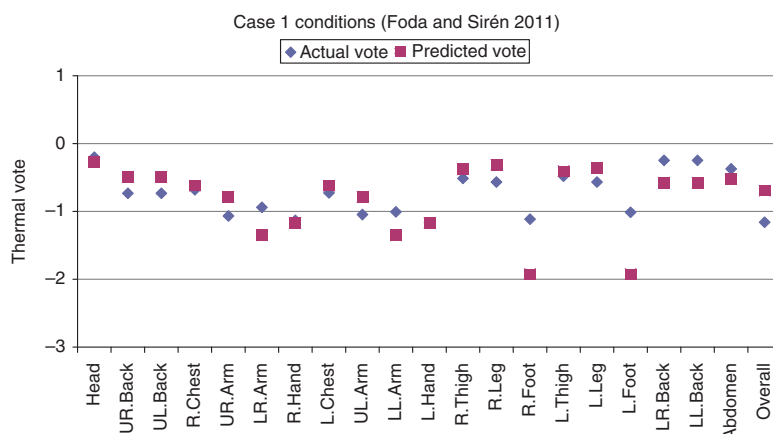
Fig. 2. Comparison between predicted votes and actual votes under Case 1 (slightly cool conditions).

Table 1 shows the regression coefficients obtained, plots of the predicted votes against the actual votes and their correlation coefficients (R^2).

The overall thermal comfort (OTC) is then estimated from the local thermal comfort (LTC) using the 7-point weighted average [23] as represented by Equation (5):

$$OTC = 0.07 * LTC_{\text{head}} + 0.35 * LTC_{\text{trunk}}$$
$$+ 0.14 * LTC_{\text{arm}} + 0.05 * LTC_{\text{hand}}$$
$$+ 0.19 * LTC_{\text{thigh}} + 0.13 * LTC_{\text{leg}} + 0.07 * LTC_{\text{foot}}$$
$$(5)$$

In Equation (5), the trunk local thermal comfort represents the average local comfort of the chest, back and abdomen, whereas the local comfort of the extremities represent the average of the right and left segments. This approach was used to account for thermal asymmetries in the space.

Model Validity

The model developed is applicable for the prediction of thermal comfort in the physiological steady-state condition under uniform or nonuniform environments. Prior to the integration with the $(ADI)_{\text{New}}$ calculations, the model was verified against subjective data in a recent study by Foda and Sirén [24]. In that study, 17 male subjects participated in the assessment of two thermally asymmetric conditions (Case 1 and Case 2). The two cases respectively represented slightly cool and slightly warm conditions. The subjects had normal office work with their own portable computers during the whole test period.

The test duration was 1 h during which the subjects reported their segmental and overall thermal votes twice. The votes were on the scale given by Nilsson [17] in the comfort zone diagram which is similar to the Bedford scale (Figure 1). Figures 2 and 3 show the predicted and actual votes under the conditions given in the two cases. As can be seen, the model's predictability based on the 7-point weighting was, in general, very good for most body segments and for the whole body. However, the model predictability was slightly lower for the feet in Case 1 (slightly cool condition) and for the hands in Case 2 (slightly warm condition).

Laboratory Measurements

Experimental Setup

The experiments were conducted in the University of Reading's environmental test chamber (Figure 4 (a)). The working compartment of the chamber has dimensions 2.78 m × 2.78 m × 2.3 m ceiling height. Two ventilation systems were tested using the chamber; mixing ventilation (MV) and displacement ventilation (DV). The mixing ventilation supply diffuser (0.4 m width and 0.01 m height) is located at the front wall (the wall facing the occupant) at a distance of 0.17 m below the ceiling. The air jet is directed towards the ceiling using a 45° deflector (Figure 4(c)). The DV diffuser has a semi-cylindrical shape with a radius of 0.25 m and a height of 0.20 m. The DV diffuser is mounted at floor level and located in the middle of the front wall (Figure 5). The test conditions were the same for both ventilation systems with an air
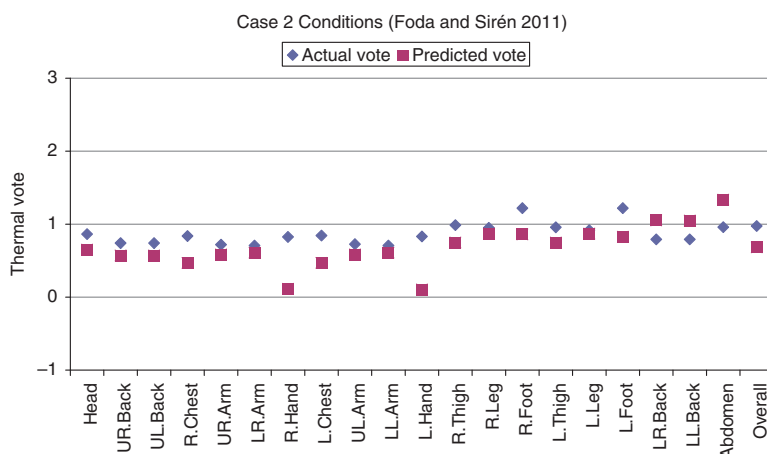
Case 2 Conditions (Foda and Sirén 2011)

◆ Actual vote ■ Predicted vote

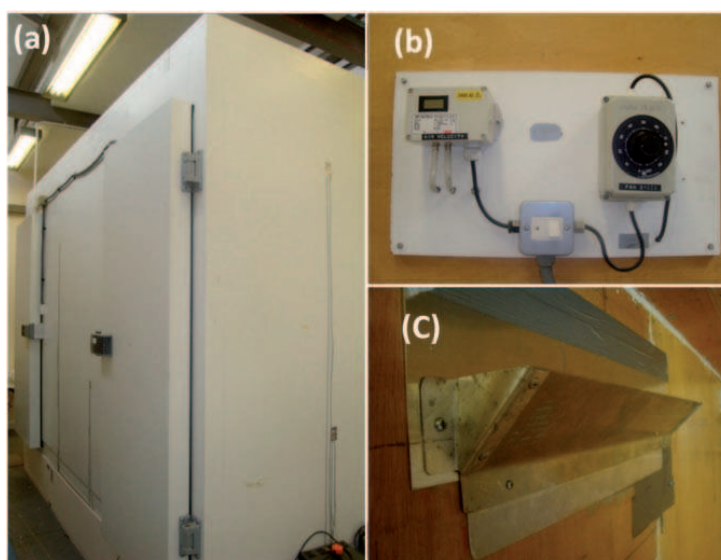**Fig. 3.** Comparison between predicted votes and actual votes under Case 2 (slightly warm conditions).

Fig. 4. (a) The environmental test chamber, (b) flow rate control panel and (c) the 45° deflector.

supply flow rate of $15\,L\cdot s^{-1}$, air supply temperature of 18°C, RH ≈ 40 % and total room load of $21.2\,W\cdot m^{-2}$ of floor area.

The physical indoor environmental parameters as well as the CO_2 concentrations were measured during the experiments. The air temperatures were measured using Platinum Resistance Thermometer (PRT) sensors with an accuracy of (± 0.15 K), air velocities were measured using

a Dantec air flow analyser (Model 54N10) with omnidirectional anemometers (accuracy 10% within the lower range of the instrument) and CO_2 concentrations were measured using a 12-channel gas analyser type Brüel & Kjaer 1302 (accuracy approximately ± 12%). Air temperatures and velocities were measured at the inlet and outlet and at the heights of 0.1, 1.1 and 1.8 m for a number of locations in the occupied zone (Figure 5). For the stand
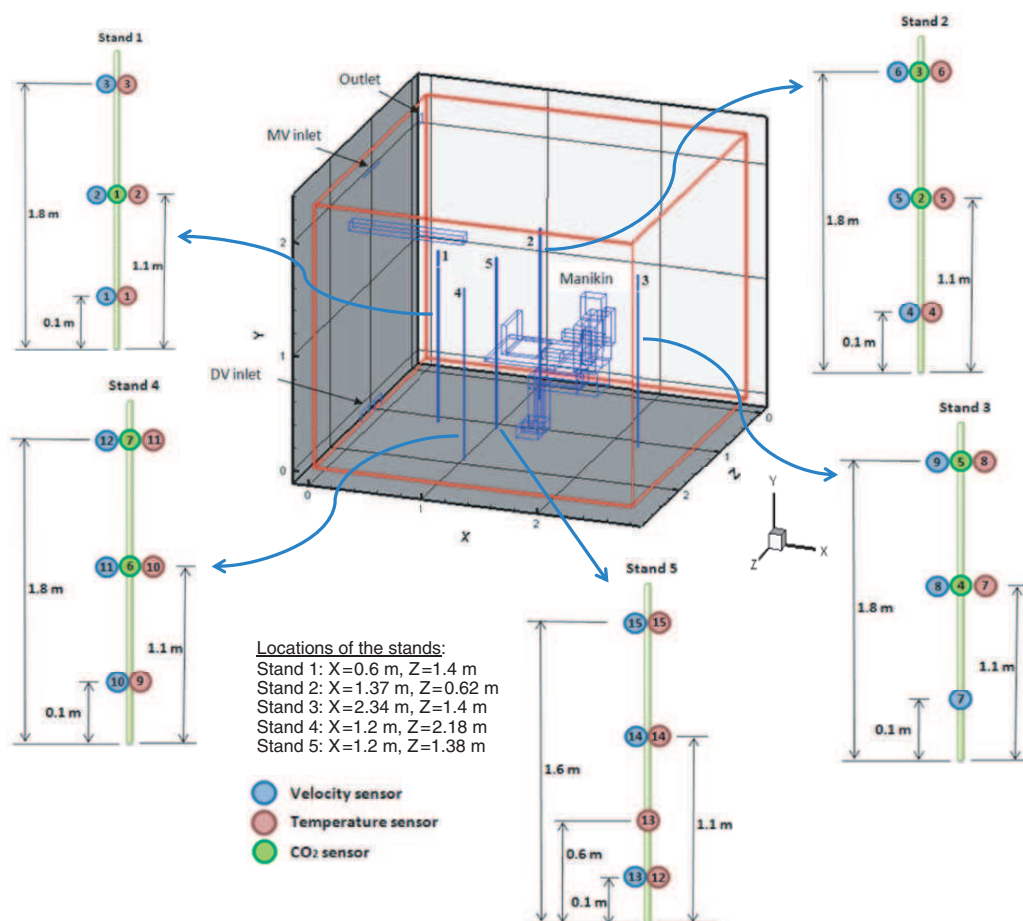
Fig. 5. The locations of temperature, velocity and CO_2 measuring points in the test chamber.

located near the occupant (i.e. stand no. 5), the air temperature was measured at four different heights (0.1, 0.6, 1.1 and 1.6 m) while the air velocity was measured at the heights of (0.1, 1.1 and 1.6 m). The CO_2 concentrations were measured at the inlet and outlet and at the heights of 1.1 and 1.8 m for many locations in the occupied zone as shown in Figure 5. The local mean age of air was measured at the breathing zone at a point located 20 cm from an occupant's nose using a standard tracer gas decay technique with SF_6 (sulphur hexafluoride) as a tracer gas. Before injecting SF_6, the ventilation system was shut down and the tracer gas was then injected in the chamber from an SF_6 cylinder and a mixing fan was kept running for 5 mins to ensure a good mixing of SF_6 in the working compartment. After that, the ventilation system was

activated and the measurements of SF_6 concentration decay commenced.

Subjects

Eight college-aged and healthy subjects (4 male and 4 female) participated in the experiments. All subjects participated in the two tests (with mixing ventilation and displacement ventilation) on two separate days. The subjects arrived at the test place 30 mins prior start of the experiment to allow sufficient time for completion of the consent form and to take his/her physical measurements (height, weight and body fat). A summary of the physical measurements of the subjects is shown in Table 2. After entering the chamber, the participants were allowed to acclimatize to the thermal environment created by the

Table 2. Anthropometric measurements of the subjects and the standard deviation

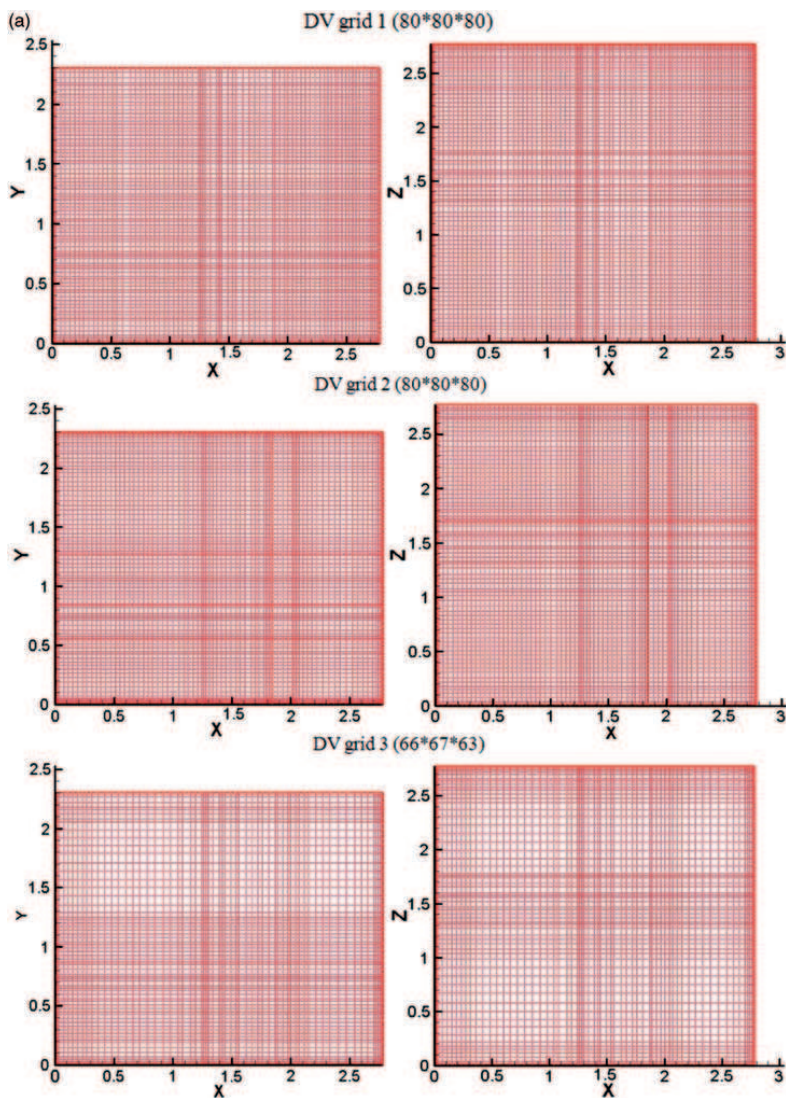| Gender	No. of subjects	Age (year)	Height (m)	Weight (kg)	Body fat (%)
Male	4	35 ± (5.48)	1.73 ± (0.06)	73.28 ± (14.21)	23.03 ± (12)
Female	4	30.25 ± (5.91)	1.65 ± (0.098)	67.6 ± (12.54)	28.68 ± (6.57)
Male & female	8	32.63 ± (5.85)	1.69 ± (0.085)	70.44 ± (12.77)	25.85 ± (9.45)

The values within brackets represent the standard deviation.

Fig. 6. Different numerical grids used for: (a) DV system (b) MV system.
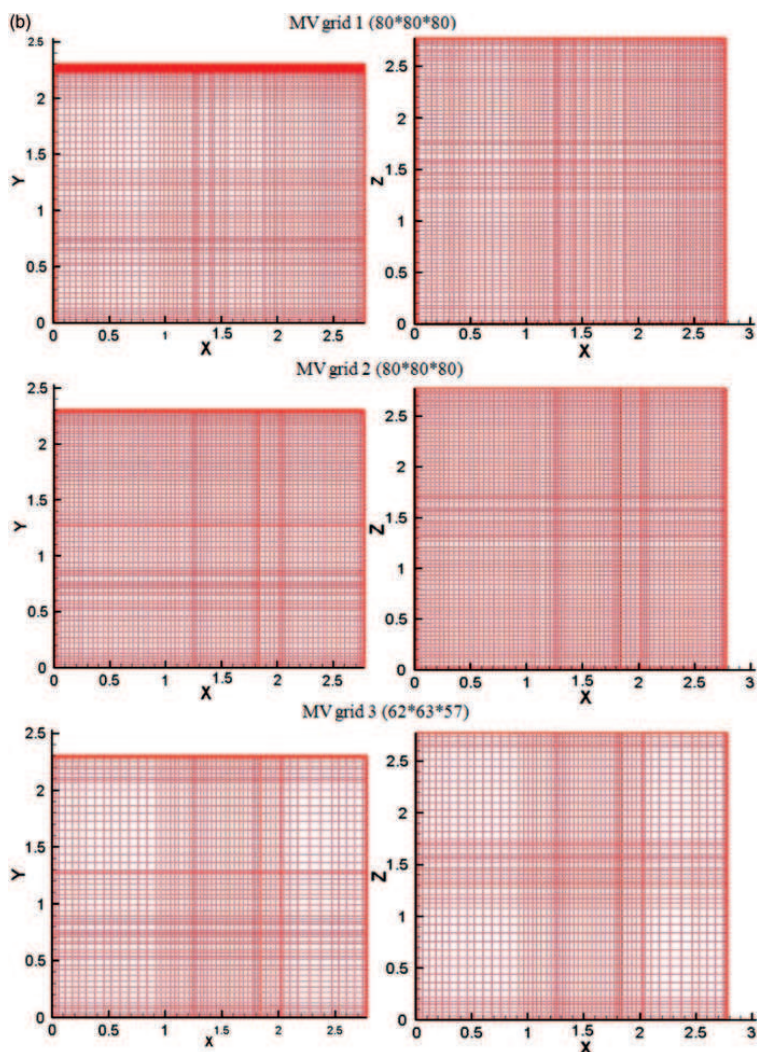
Fig. 6. Continued.

ventilation systems for 30 mins before commencing the tests. In the main tests, the subjects sat at a desk facing the diffuser (Figure 5) and performed sedentary activities such as reading or using a laptop and were not allowed to move inside the chamber. The subjects were exposed to the thermal environment for 2 h and had been asked to fill in a questionnaire every 15 mins to rate their local and overall thermal sensation levels based on the 7-point ASHRAE scale. All participants wore an ensemble of typical office clothing consisting of long sleeve shirt, cotton undershirt (T-shirt), trousers, pants and athletic socks. Female subjects wore bra instead of underwear cotton T-shirt. The estimated overall clo value for the male clothing ensemble was 0.72 while the estimated one for the female clothing ensemble was 0.64.
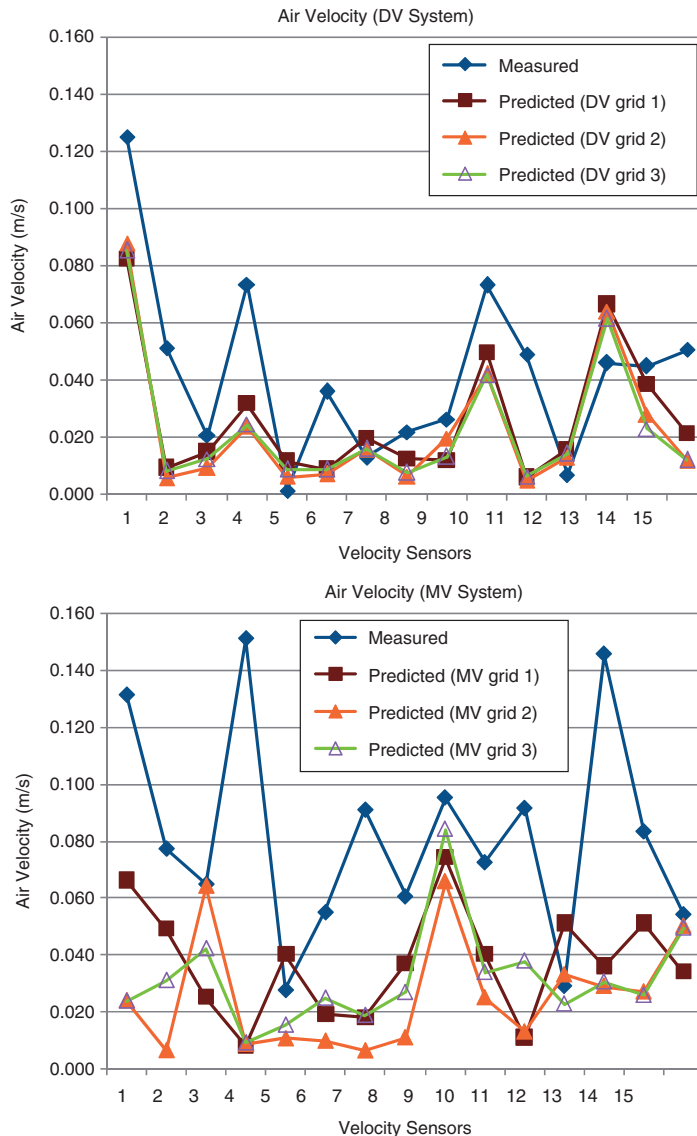
Fig. 7. The measured and predicted velocities using different numerical grids for the DV and MV systems.

CFD Simulations

CFD technique has progressed during the last few decades and has been proven to be a powerful and efficient tool for simulating air flow and contaminant dispersion in indoor environments [10]. The numerical calculations to predict the airflow properties in the chamber were carried out using the CFD code VORTEX 4.0 [19]. This program has been developed for the simulation of airflow, heat transfer, concentration and mean age of air distribution in indoor environments. The code uses the standard $k - \varepsilon$ and the Renormalization Group (RNG) $k - \varepsilon$ turbulence models and has been developed for ventilation research, which may be more suitable for ventilation simulation than other general-purpose codes.

For the CFD simulations, three different numerical grids have been tried for both the DV and MV systems;
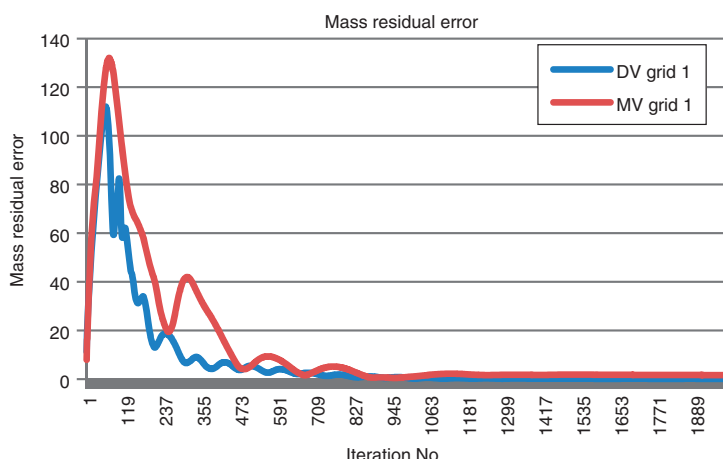
Fig. 8. Mass residual errors for DV grid 1 and MV grid 1.

DV grid 1, DV grid 2, DV grid 3, MV grid 1, MV grid 2 and MV grid 3. All these grids are 3-D structured Cartesian grids with 80*80*80 points (in x, y and z direction) for DV grid 1, DV grid 2, MV grid 1 and MV grid 2, 66*67*63 points for DV grid 3 and 62*63*57 points for MV grid 3. Although DV grid 2 and MV grid 2 have the same grid points as DV grid 1 and MV grid 1 (i.e. 80*80*80), they have a different configuration (Figure 6).

When comparing the predicted air velocities using the grids mentioned earlier with the measured ones (Figure 7) it is quite obvious that DV grid 1 and MV grid 1 provide better results than the other grids. Also, the solutions converged better when using DV grid 1 and MV grid 1 (Figure 8). Therefore, DV grid 1 and MV grid 1 have been used in the current study to simulate the air flow pattern in the environmental test chamber that was created by the two ventilation systems.

The equations for the momentum, energy, concentration, kinetic energy and turbulent dissipation rate are discretised using a HYBRID scheme. The pressure–velocity coupling algorithm SIMPLE was used to solve the continuity equation and the RNG $k - \varepsilon$ model was used to represent the turbulent behaviour of the flow within the chamber. The near wall nodes were located 5 mm from the wall surfaces as this is the optimum distance to use as recommended by Awbi [25].

The geometry of the MV inlet used in the CFD simulations is a simple rectangular opening which has a width of 0.4 m and a height of 0.01 m. This geometry is exactly the same as the MV inlet slot used in
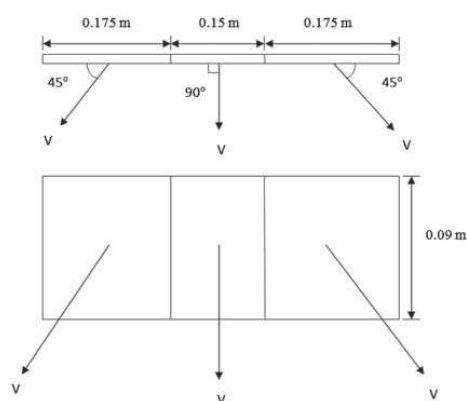

Fig. 9. The simulated DV inlet diffuser used in VORTEX code.

the experiments. It is worth mentioning that the calculated flow rate using the simulated MV inlet diffuser is exactly the same as the measured one. For the DV inlet diffuser, since it is not possible to use a curved grid in the VORTEX code to represent the semi-cylindrical shape, the DV inlet was simulated using a rectangular opening. To allow for the radial air flow distribution for this diffuser, the rectangular opening was divided into three sections as shown in Figure 9. For the middle section, the direction of the air flow is perpendicular to the inlet surface while for the left and the right sections, the air flow is inclined by an angle of $45°$ to the central part of the diffuser.
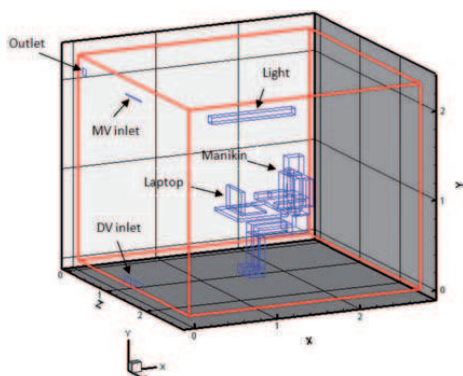

A New Room Air Distribution Index

Indoor Built Environ 2012;000:1–22

13

Fig. 10. The virtual manikin used in the CFD simulations.

Table 3. The surface area of the individual segments of the virtual manikin

Body part	Surface area (m^2)
Head	0.1596
Chest	0.2328
Back	0.2388
Pelvis	0.2460
Upper arm (2 segments)	0.1671
Lower arm (2 segments)	0.1298
Hand (2 segments)	0.1045
Thigh (2 segments)	0.3757
Leg (2 segments)	0.2590
Foot (2 segments)	0.1293
Whole body	2.0426

The geometry of the simulated DV diffuser, which has been adjusted to give the same flow rate as the measured one, has a width of 0.5 m and a height of 0.09 m.

The occupant's presence in the room was simulated using a virtual thermal manikin (Figure 10). The virtual manikin has a cubical shape and formed, as much as possible, to have the same size and area as those corresponding to the thermal manikin "Therminator" [24]. The total surface area of the clothed manikin is 2.043 m^2. Table 3 shows the surface area of the individual segments of the virtual manikin. The rate of CO_2 production in humans used in the CFD simulations was estimated using Equation (6) [10]:

$$G = 4 * 10^{-5} * M * A \qquad (6)$$

Where G is the CO_2 production per person (L·s^{-1}), M is the metabolic rate (W·m^{-2}) and A is the body surface

area (m^2). The body surface area is calculated using Equation (7) [26]:

$$A = 0.203 * Ht^{0.725} * Wt^{0.425} \qquad (7)$$

where Ht is the body height (m) and Wt is the body weight (kg). In this study, the average height and weight for the occupants was 1.69 m and 70.44 kg, respectively. The estimated CO_2 production per person used in the CFD simulations was 0.00464 L·s^{-1} based on assumed metabolic rate for the sedentary activity (i.e. 1.1 met = 64 W·m^{-2}).

The data for the boundary conditions that were based on laboratory measurements and used in the simulations related to the temperatures of the chamber's six surfaces; inlet air velocity, temperature, CO_2 concentration and turbulence intensity; appliance's heat flux; and the light fixture's surface temperature. The boundary conditions for the virtual manikin were predicted using the MS-Pierce model and were assigned to each body segment. This included the segmental heat fluxes and the clothed body temperatures. In order to predict these quantities in the concurrent simulations with the shortest time possible, the MS-Pierce thermoregulation model was fed with the measured environmental physical parameters at different heights (i.e. air temperature, air velocity, radiant temperature, relative humidity) together with the personal data (i.e. clothing insulation and metabolic rate).

Results and discussion

Thermal Comfort
The predicted local comfort votes from the simulations along with the actual subjective votes are shown in Figures 11 and 12 for the two cases of the DV and MV systems respectively. The figures show the predicted and actual votes for the head, chest, back, pelvis and the right-side body limbs as well as for the whole body. The differences between the actual and predicted votes under the test conditions by the DV and the MV systems were not significant for most body segments. The actual votes were the average from all subjects' votes (4 male and 4 female). The test conditions in the chamber for both ventilation methods produced almost neutral conditions ($T_m = 25.5°C$ and 25.3°C for DV and MV, respectively). Therefore, the difference in the average overall sensation votes for the two test conditions was not significant and was nearly consistent with the planned condition (i.e. neutral). However, in the DV tests the subjects felt slightly cooler especially for the lower extremities when compared with
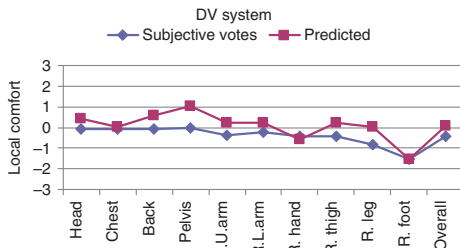
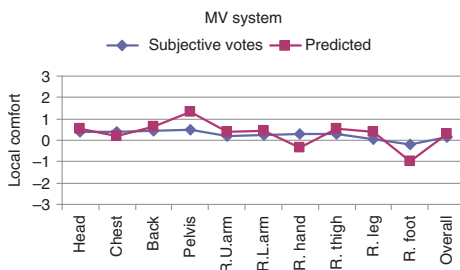**Fig. 11.** Predicted and actual votes for the exposure to the DV system.

Fig. 12. Predicted and actual votes for the exposure to the MV system.

the MV tests and this consequently slightly affected their overall sensations. This may be related to the temperature stratification in the chamber where the lower parts of the subjects' bodies were subjected to lower temperatures.

The predicted votes were in good agreement with the actual votes for most body parts under the two test conditions (DV and MV systems). The maximum deviation was <1 on the comfort scale at the pelvis segment for the exposure with the DV system and at the foot segment for the exposure with the MV system. The subjective votes in these tests were based on the ASHRAE 7-point scale while the comfort model was based on the Bedford 7-point scale. However, the difference between the two scales is believed to be very minor in the range close to the neutral sensations (i.e. from −1 to 1) which is perceived under these two exposures.

Room Physical Parameters

The predicted air velocity, temperature and CO_2 concentration profiles are presented in Figures 13–16. Figure 13 shows the air velocity profile in a vertical plane

located in the middle of the chamber where the manikin is seated. There was no sign of draft observed around the manikin or in the occupied zone for both ventilation systems. The only high air velocity region was near the ceiling for the case of mixing ventilation. This region of high air velocity was generated by the air jet supply from the wall diffuser which then decreased as the flow progressed towards the opposite wall. However, to observe the plumes around the manikin, the contour plot scale was selected to be from 0 to $0.2 \, \text{m} \cdot \text{s}^{-1}$.

Figure 14 shows the air temperature contours at planes of heights of 0.1, 0.6 and 1.1 m. It is clear from Figure 14 that the air temperatures for the DV system at these levels were in general lower than those for the MV system. The predicted air temperatures at these levels (0.1, 0.6 and 1.1 m) and 0.1 m away from the corresponding body segments (i.e. ankle, abdomen and head) were 22.4, 27.2 and 26.8°C respectively for the DV system and 25.1, 28.6 and 27°C respectively for the MV system. The thermal plumes from heat sources (i.e. manikin and laptop) are shown in Figure 15. As can be seen, the lower air temperatures were near the inlet diffusers which then increased gradually until they reached maximum values around the heat sources.

Figure 16 shows the CO_2 concentration in (ppm) at a plane located in the middle of the chamber. The CO_2 concentration in the occupied zone was more stratified and showed lower values for the DV system case compared with the MV system. Clearly this suggests that the DV system provided better air quality in the occupied zone than in the MV system. The maximum CO_2 concentration for both systems was located at the breathing zone which is the source of the CO_2 production.

A comparison between the predicted and measured air temperatures, velocities and CO_2 concentrations at different locations in the occupied zone is shown in Figure 17. The air temperature, velocity and CO_2 sensors are located on the five stands shown in Figure 5.

As can be seen from Figure 17, the predicted and measured air velocities for DV system were generally in good agreement with some minor discrepancy especially at the measuring point nos 1, 2, 4 and 11. In contrast, the discrepancy between the predicted and measured air velocities is noticeable for the MV system at some measuring points. However, for the locations where the measured air velocity is lower than $0.1 \, \text{m} \cdot \text{s}^{-1}$, the discrepancy could be due to the velocity sensors' large uncertainty for velocities below $0.1 \, \text{m} \cdot \text{s}^{-1}$. Whilst for the locations where the measured air velocity is greater than $0.1 \, \text{m} \cdot \text{s}^{-1}$ (e.g. measuring point nos 1, 4 and 13
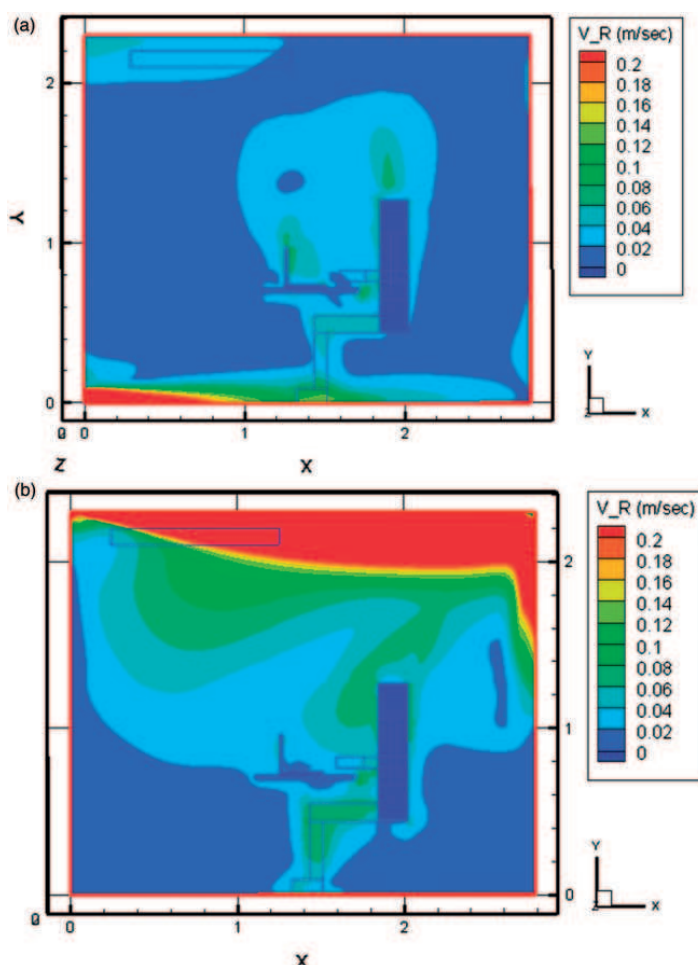
Fig. 13. Velocity contour plots at a plane located in the middle of the chamber (a) DV system (b) MV system.

for the MV system, which are located a distance of 0.1 m from the floor surface), the discrepancy could be attributed to disturbance of the air flow at these locations of the test chamber resulting from the dense sensors' wiring close to the floor level.

The predicted and measured air temperatures were in good agreement. The difference between the predicted and measured temperatures was in a range from −0.08 to 0.97 K for the DV system and from −0.03 to 0.8 K for the MV system. While most of the predicted CO_2 concentrations were overestimated, the percentage difference between measured and predicted concentration was in
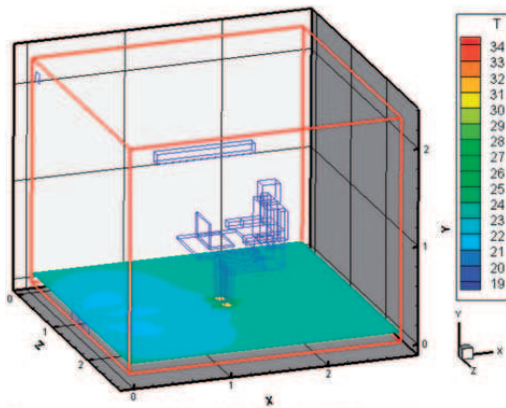
the range from 0.13% to 11.09% for the DV system and from 0.78% to 10.4% for the MV system.

In general, the minor discrepancies between the predicted and measured quantities may be related to the simplifications in the modelling of the real enclosure and/ or due to measurement errors.
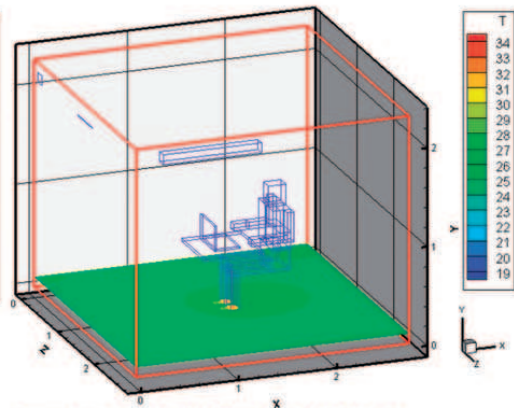
Assessment of the Performance of Ventilation Systems using $(ADI)_{New}$

The measured mean air temperature in the occupied zone, which was used to calculate ε_t, represents an average of the measurements from 15 temperature sensors
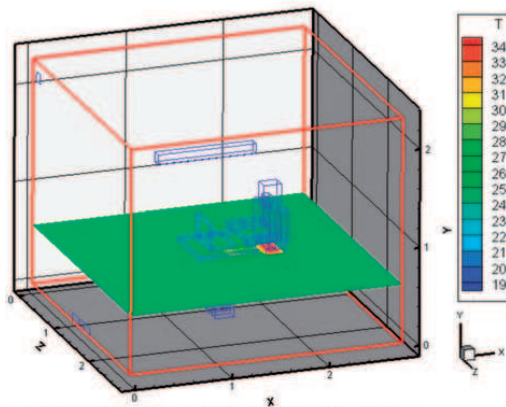

Fig. 14. Temperature contour at different heights (0.1, 0.6 and 1.1 m) for both the DV and MV systems.

Fig. 15. Thermal plumes from heat sources for the DV and MV systems.
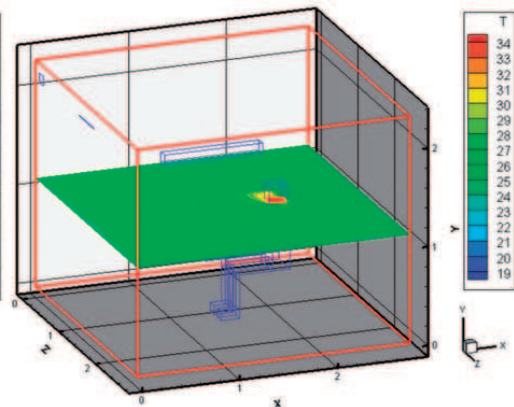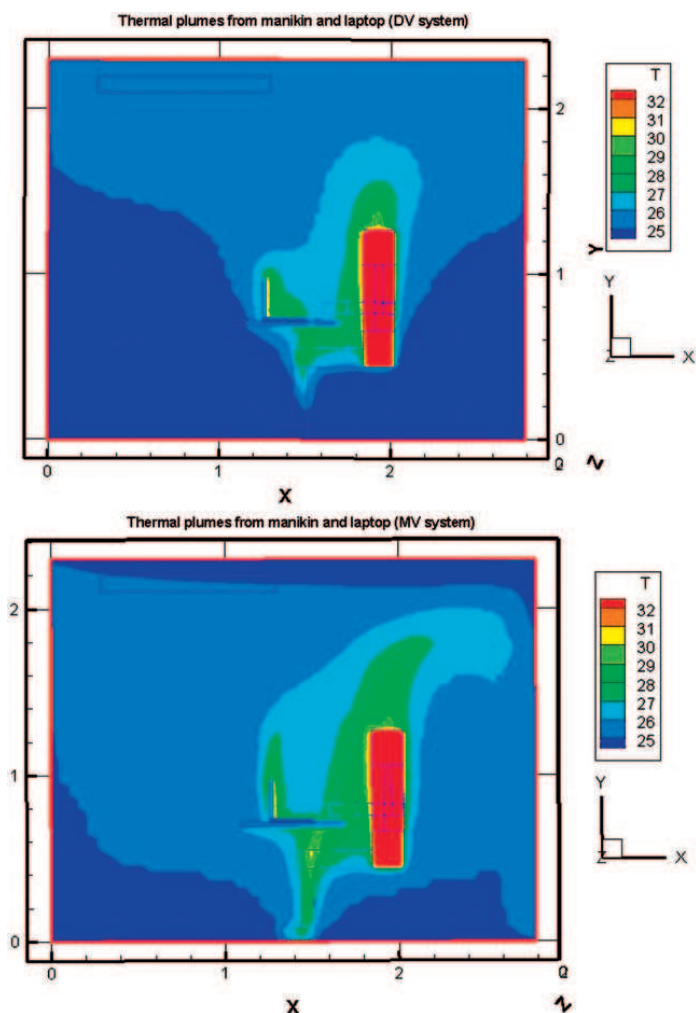
distributed in the occupied zone for the last 1 h of the recorded data. Similarly, the measured mean CO_2 concentration, which was used to calculate ε_c, represents an average of the measurements by seven CO_2 sampler points in the occupied zone for the last 1 h of the recorded data.

Although the occupants' thermal sensation from the subjective votes ($|S|$) for the MV system was slightly better than that for the DV system, the DV system produced better thermal comfort number ($N_{T.C.}$) and

this is related to its better performance in heat removal from the occupied zone (represented by ε_t) compared with the MV system. Moreover, for the DV system case, the air flow was supplied directly to the occupied zone close to the floor level which was then entrained by plumes rising from the heat sources in the chamber due to buoyancy. This air flow mechanism of the DV system makes it more efficient in removing contaminants (represented by ε_c) from the occupied zone as well as delivering fresh air to the breathing zone in less

CO₂ concentration contour at a plane located at the middle of the chamber (DV system).

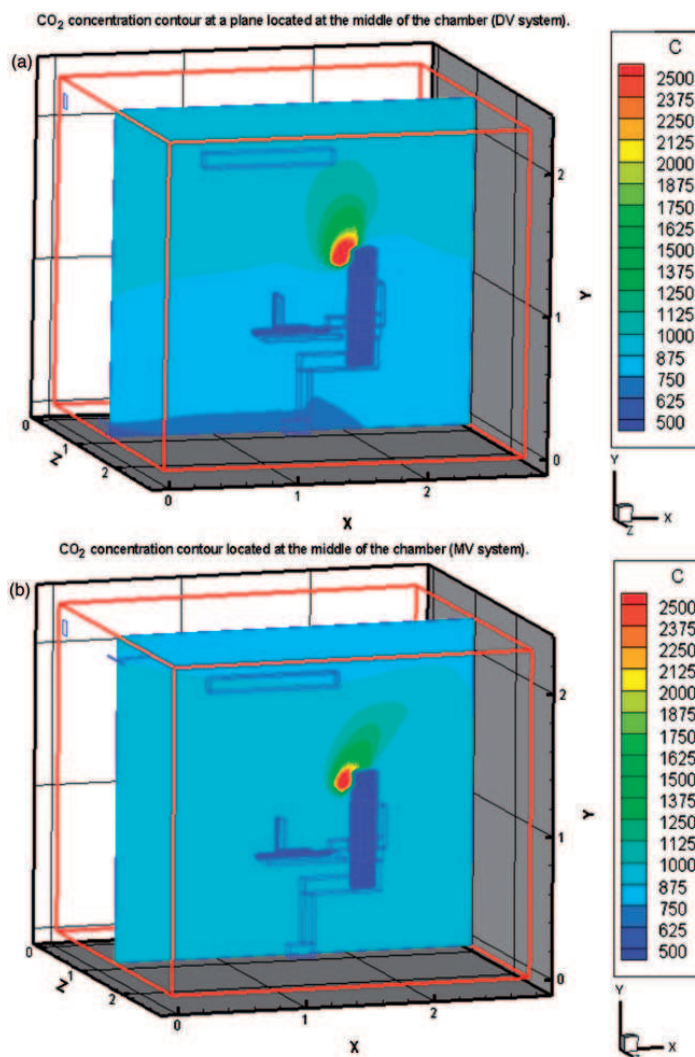CO₂ concentration contour located at the middle of the chamber (MV system).

Fig. 16. CO_2 concentration in (ppm) at a plane located in the middle of the chamber (a) DV system, (b) MV system.

time than that for the MV system. As a result, the DV system showed better air quality number ($N_{A.Q.}$) compared with the MV system and consequently better (higher) $(ADI)_{New}$ value as shown in Table 4. The differences between the DV and MV systems found in this study are in general agreement with those found in previous studies [2,27,28].

Table 4 shows the thermal comfort and air quality numbers used in calculating $(ADI)_{New}$ for both ventilation

systems along with the other parameters that were based on the predicted and measured (or subjective) quantities. As can be seen from Table 4, the differences between the predicted and measured quantities used for the calculation of $(ADI)_{New}$ were not significant. Consequently, the differences between the $(ADI)_{New}$ values based on the CFD predictions and those based on the measured (or subjective) quantities were minor. Based on this comparison, therefore, it may be concluded that the simulation
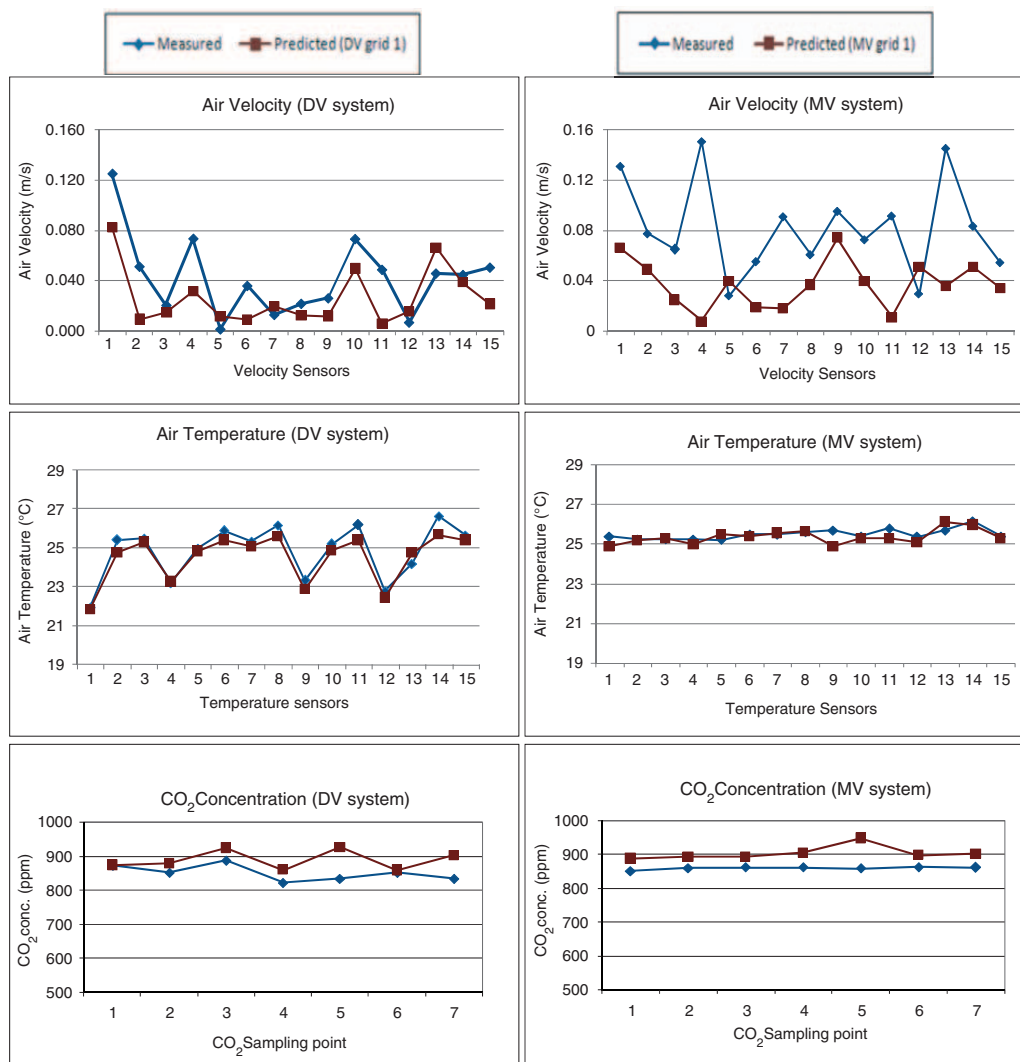
Fig. 17. The predicted and measured air velocities, temperatures and CO_2 concentrations for the DV and MV systems.

Table 4. Comparison between measured and calculated air distribution index $(ADI)_{New}$.

System		$|S|$	ε_t	$N_{T.C.}$	τ_n (h)	$\bar{\tau}_p$ (h)	ε_c	$N_{A.Q.}$	$(ADI)_{New}$
MV	Measured/Subjective	$|0.14 \pm 0.51|$	0.95	0.91	0.33	0.57	1.04	0.60	1.51
	Predicted	$|0.31|$	0.96	0.86	0.33	0.59	0.91	0.51	1.37
DV	Measured/Subjective	$|-0.43 \pm 0.38|$	1.13	0.97	0.33	0.49	1.10	0.74	1.71
	Predicted	$|0.07|$	1.14	1.11	0.33	0.66	1.10	0.55	1.66

The values after ($\pm$) sign represents the standard deviation.
The predicted $|S|$ is calculated using the proposed overall thermal comfort model *(OTS)* (Equation (5)).

tool used in this study provides a sufficiently accurate prediction for the assessment of ventilation systems.

Conclusions

This study introduced a new air distribution index $(ADI)_{New}$ to assess the indoor thermal comfort and air quality that is applicable for uniform and nonuniform thermal environments. The overall thermal comfort assessment used in calculating $(ADI)_{New}$, was based on the local thermal comfort concept. This was carried out using a weighted average of the local thermal comfort perceived by the different body segments. The local thermal comfort was predicted using a model that was adapted for use with the MS-Pierce thermoregulation model and based on the structure of the UCB comfort model. This index was used in the present study to compare the performance of two well-known ventilation systems, MV and DV systems, with both CFD simulations and laboratory-based measurements. Based on the predicted and the measured data, the DV system showed better thermal comfort and air quality numbers compared with the MV system and consequently better (higher) $(ADI)_{New}$ value.

The CFD simulations were carried out to calculate the parameters used in calculating the value of $(ADI)_{New}$, such as the ventilation effectiveness for heat removal (ε_t), the ventilation effectiveness for contaminant removal (ε_c) and the local mean age of air ($\bar{\tau}_p$). In general, the predicted parameters were in good agreement with the measured ones. Since the experimental measurements are quite expensive and time consuming, the implementation of CFD with a thermoregulation thermal comfort model is faster and more cost-effective and can be considered as a powerful tool for assessing the performance of ventilation systems. The initial validation of this combination of simulation tools (i.e. CFD and thermoregulation thermal comfort models) is promising. However, further validations are needed before extensive application of this simulation tool could be made. Although the analysis was based on a relatively small test chamber, the new index would also be applicable to larger spaces representing actual buildings where variations in indoor environment parameters could be larger than what was experienced in this chamber study. For such large indoor spaces with many occupants, $(ADI)_{New}$ should be calculated at different locations.

References

1 Gan G: Numerical investigation of local thermal discomfort in offices with displacement ventilation: Energ Build 1995; 23: 73–81.

2 Lin Z, Chow TT, Fong KF, Wang Q, Li Y: Comparison of performances of displacement and mixing ventilations. Part I: Thermal comfort: Int J Refrig 2005; 28: 276–287.

3 Pan CS, Chiang HC, Yen MC, Wang CC: Thermal comfort and energy saving of a personalized PFCU air-conditioning system: Energ Build 2005; 37: 443–449.

4 Yang X, Srebric J, Li X, He G: Performance of three air distribution systems in VOC removal from an area source: Build Environ 2004; 39: 1289–1299.

5 Cheong KWD, Yu WJ, Tham KW, Sekhar SC, Kosonen R: A study of perceived air quality and sick building syndrome in a field environment chamber served by displacement ventilation system in the tropics: Build Environ 2006; 41: 1530–1539.

6 Dascalaki EG, Lagoudi A, Balaras CA, Gaglia AG: Air quality in hospital operating rooms: Build Environ 2008; 43: 1945–1952.

7 Cho Y, Awbi HB, Karimipanah T: Theoretical and experimental investigation of wall confluent jets ventilation and comparison with wall displacement ventilation: Build Environ 2008; 43: 1091–1100.

8 Awbi HB, Gan G: Evaluation of the overall performance of room air distribution: in Proceedings of Indoor Air'93, The 6th International Conference on Indoor Air Quality and Climate, 4–8 July 1993, Helsinki, Finland; Vol 5, pp. 283–288.

9 Awbi HB: Energy efficient room air distribution: Renew Energ 1998; 15: 293–299.

10 Awbi HB: Ventilation of Buildings. London, Spon Press, Taylor & Francis Group, 2003.

11 Karimipanah T, Awbi HB, Sandberg M, Blomqvist C: Investigation of air quality, comfort parameters and effectiveness for two floor-level air supply systems in classrooms: Build Environ 2007; 42: 647–655.

12 Fanger PO: Thermal Comfort. Copenhagen, Danish Technical Press, 1970.

13 Wyon DP, Larsson S, Forsgren B, Lundgren I: Standard procedures for assessing vehicle climate with a thermal manikin: SAE Paper 890049, 1989.

14 Zhang H: Human thermal sensation and comfort in transient and non-uniform thermal environments. PhD thesis, The University of California, Berkeley, CA, 2003.

15 Foda E, Almesri I, Awbi HB, Sirén K: Models of human thermoregulation and the prediction of local and overall thermal sensations: Build Environ 2011; 46: 2023–2032.

16 Foda E, Sirén K: A new approach using Pierce two-node model for different body parts: Int J Biometeorol 2011; 55(4):519–532.

17 Nilsson H: Comfort climate evaluation with thermal manikin methods and computer simulation models. PhD thesis, University of Gävle, Sweden, 2004.

18 Cheong KWD, Yu WJ, Sekhar SC, Tham KW, Kosonen R: Local thermal sensation and comfort study in a field environment chamber served by displacement ventilation system in the tropics: Build Environ 2007; 42: 525–533.

19 Awbi HB: VORTEX: A computer code for airflow, heat transfer and concentration in enclosure. Version 4D-RNG, Reading, UK, 2005.

20 Awbi HB: Energy efficient ventilation for retrofit buildings: in Proceedings of 48thAiCARR International Conference on Energy Performance of Existing Buildings, 22–23 September 2011, Baveno, Italy, pp. 23–46.

21 Almesri I, Awbi HB: Evaluation of air distribution systems using a new air distribution index: in Proceedings of Indoor Air 2011, 12th International Conference on Indoor Air Quality & Climate, 5–10 June 2011, Austin, Texas, USA, Paper a1004-5.

22 Gagge AP, Fobelets AP, Berglund LG: A standard predictive index of human response

to the thermal environment: ASHRAE Trans 1986; 92(2): 709–731.

23 Hardy JD, DuBois EF: The technique of measuring radiation and convection: J Nutr 1938; 15(5): 461–475.

24 Foda E, Sirén K: A thermal manikin with a human thermoregulatory control – Implementation and validation: Int J Biometeorol 2011. DOI: 10.1007/s00484-011-0506-6.

25 Awbi HB: Calculations of convective heat transfer coefficients of room surfaces for natural convection: Energ Build 1998;28:219–27.

26 Dubois D, Dubois EF: A formula to estimate the approximate surface area if height and weight be known: Arch Intern Med 1916; 17:863–871.

27 Lin Z, Chow TT, Fong KF, Tsang CF, Wang Q: Comparison of performances of displace-ment and mixing ventilations. Part II: Indoor air quality: Int J Refrig 2005; 28: 288–305.

28 Cho Y, Awbi HB, Karimipanah T: A compar-ison between four different ventilation systems: in Proceedings of Roomvent 2002, the 8th International Conference on Air Distribution in Rooms, 8–11 September 2002, Copenhagen, Denmark, pp 181–184.